Quantum Oscillations in the Layer Structure of Thin Metal Films

P. Czoschke, H. Hong, L. Basile, T.-C. Chiang
Materials Research Laboratory (MRL), University of Illinois at Urbana-Champaign (UIUC), Urbana, IL, U.S.A.

Introduction

As the physical size of a structure approaches the atomic scale, nonclassical effects become increasingly important, and departure from the bulk properties can be expected. In particular, quantum electronic effects have been shown to play an important role in determining the growth behavior and morphology of metal films. Given the importance of electronic effects in these systems, it has been predicted that quantum size effects will manifest themselves in the layer structure of the film as well, causing variations in the atomic interlayer spacings [1]. However, evidence for such effects has been limited to the measurement of step heights by scanning tunneling microscopy (STM) and helium atom scattering (HAS) [2-4], both of which probe only the top surface of the film and provide little information on internal film structure.

Here we present a surface x-ray diffraction study of smooth Pb films deposited on a Si(111) substrate. Since x-rays fully penetrate the film, information on the internal atomic layer structure as well as on the buried film/substrate interface is probed. The results show lattice distortions with a quasi-bilayer periodicity, which can be explained with a physical model based on confinement of the film's conduction electrons to a quantum well and interference effects between the film boundaries. The absolute film thicknesses are also determined. They indicate the presence of substantial oscillatory step-height variations on the film surface.

Methods and Materials

We determined the interlayer spacings in the metal films by measuring, *in situ*, the integrated specular reflectivity rod by using 19.9-keV x-rays from an undulator source at UNI-CAT beamline 33-ID at the APS. The substrate was prepared by depositing 4.5 Å of Pb onto a clean Si(111)-(7×7) reconstructed surface at room temperature, followed by a 10-minute anneal at 415°C. This process results in the 1/3 monolayer (ML) coverage, commensurate with Pb/Si(111)-$(\sqrt{3} \times \sqrt{3})$R30° surface [5, 6], which was verified by examining reflection high-energy electron diffraction (RHEED) patterns, in-plane x-ray superstructure peaks, and the x-ray reflectivity rod. Pb films were deposited incrementally by using an effusion cell at a rate of 0.652 Å/min, which was calibrated by using a quartz crystal thickness monitor. The sample temperature was maintained at 110K for the duration of the experiments and measured via a thermocouple attached to the clips holding the sample. The specular rod profile was measured by using either the ω-scan method or a series of parallel line scans to obtain the background-subtracted integrated intensity. Different momentum transfers were selected by varying the incident beam angle and exiting scattering angle with a six-circle diffractometer that was integrated with the ultrahigh vacuum chamber used to prepare the sample.

Results

The extended reflectivity profiles for nominal coverages N = 6-18 Pb MLs are shown in Fig. 1. The steep tails at perpendicular momentum transfer $l = 3$ and 9 are the edges of the Si(111) and (333) Bragg peaks, respectively, between which are multilayer interference fringes due to the Pb overlayers. ML resolution is evident as some of the interference minima turn into near maxima with a ML increment in film thickness. These results imply that the films follow a smooth, layer-by-layer growth mode, which is in stark contrast to the "magic thickness" effect seen for growth at higher temperatures [7].

The most unusual features of the profiles in Fig. 1 are the relatively pronounced fringes at $l \approx 4.8$ and 8.1, marked by inverted triangles, which are located approximately halfway between the bulk Pb(111), (222), and (333) Bragg positions at $l = 3.3$, 6.6, and 9.9, respectively. The proximity of the features to the half-order point for Pb is an indication of a quasi-bilayer superperiodicity to the lattice in the *z* direction (the surface normal). This effect is analogous to the superstructure peaks found at in-plane fractional order positions due to surface reconstructions. However, in our case the superperiod, or periodic lattice distortion, is in the direction of the surface normal. The intensity of the superstructure peak is much lower than the Pb Bragg peaks, indicating that the quasi-bilayer distortion is relatively weak and possibly damped. Damping is also implied because bulk Pb does not exhibit such distortions.

The quasi-bilayer lattice distortion can be explained in terms of electronic charge density variations in the film by recognizing that confinement of the conduction electrons in the metal film by its boundaries leads to a 1-D quantum well. As a result, the charge density in the film differs from the perfectly periodic bulk charge density. A charge imbalance or asymmetry about an atomic plane exerts an electronic force that can move the atomic plane away from the ideal bulk position. By making the approximation that the itinerant electrons in

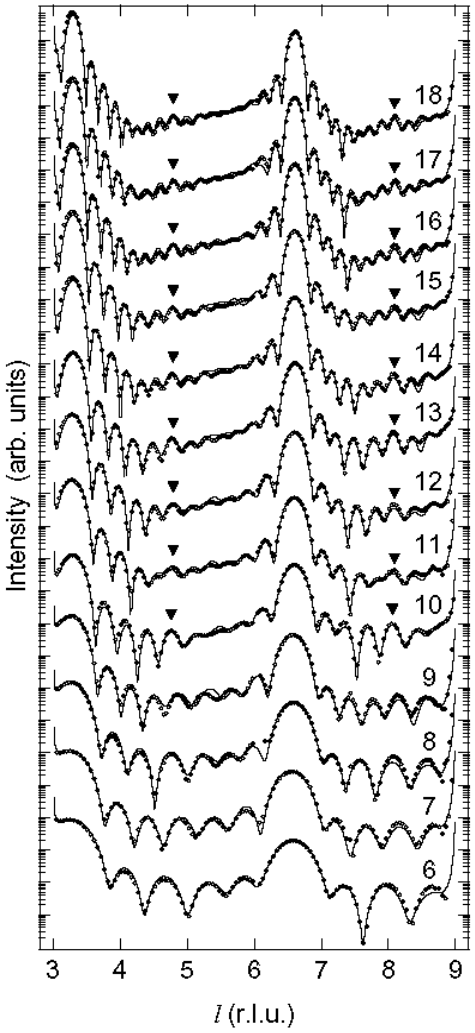

FIG. 1. Extended x-ray reflectivity data (circles) for Pb films with thicknesses of 6-18 ML and fits from using a model incorporating quantum oscillations in the electronic charge density (solid curves). Nominal coverages are indicated for each curve. The abscissa is the momentum transfer along the surface normal in Si reciprocal lattice units (1 r.l.u. = 0.668 Å^{-1}). The tails of the sharp Si(111) and (333) Bragg peaks can be seen at l = 3 and l = 9, and the large peaks at l ≈ 3.3, 6.6, and 9.9 (not shown) correspond to the Pb(111), (222) and (333) Bragg positions, respectively, halfway between which the prominent half-order features can be seen (inverted triangles). As discussed in the text, such features are indicative of a quasi-bilayer superperiod in the direction normal to the surface.

the Pb film form a free-electron gas, a simple model can be developed to yield a closed form expression for the free-electron charge density as a function of depth into the film. Within a linear response regime appropriate for small lattice distortions, the movement of an atomic plane is proportional to the derivative of the local charge density. Such a model gives rise to a n_0-slit interference pattern in the charge density with a characteristic wavelength of $D/n_0 \approx \pi/k_F = \lambda_F/2$ (one-half of the Fermi wavelength). An example of this effect for one of the films here studied, with $N = 10$, can be seen in the top panel of Fig. 2. The oscillations are similar to the usual Friedel oscillations. They are damped away from the boundaries, but there is considerable interaction (or

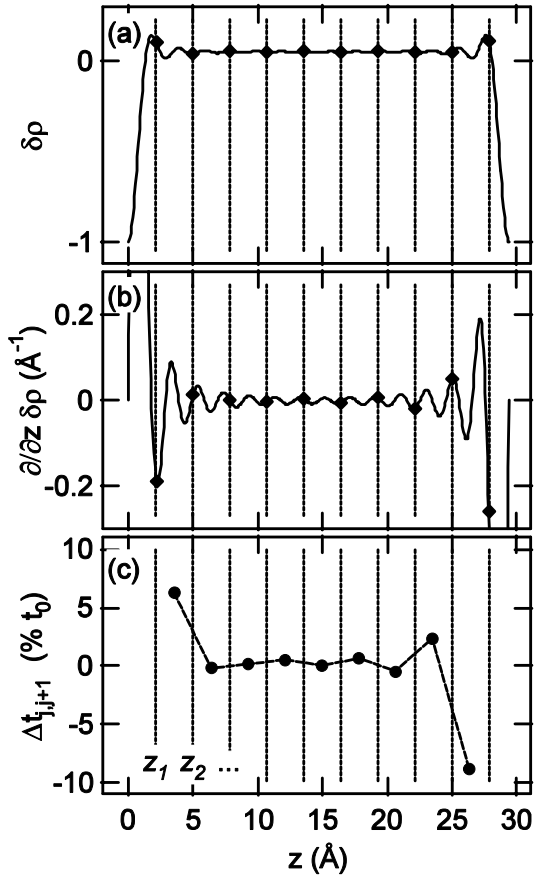

FIG. 2. Due to the confinement of conduction electrons in a quantum well (N = 10), oscillations in the electron density (a) will be present in the film. The displacement of each atomic plane is proportional to the first derivative (b) of these density variations, from which the changes in individual interlayer spacings (c) can be calculated. The abscissa is the distance into the quantum well, where z = 0 is the film/substrate well boundary. The ideal positions of the atomic layers z_j are marked with vertical dotted lines, and in panels (a) and (b), the intersection of these positions with the curves are marked with diamonds. All curves and values are calculated by using the model parameters resulting from the fit to the experimental data for N = 10 shown in Fig. 1.

interference) between the two boundaries for the thickness ranges investigated here.

The experimental data in Fig. 1 were fit by using a standard kinematic model [8-10], with the lattice distortion given by the aforementioned model. Film roughness is allowed in the model as a distribution of thicknesses but is fairly small from the fits. The calculated reflectivity profiles based on the model are shown in Fig. 1 as solid curves. They describe the data very well over the wide thickness range, and, most importantly, they reproduce the half-order features discussed above.

Discussion

The model thus reproduces the quasi-bilayer periodicity in the film structure. A physical explanation follows. In addition to the charge density variations, Fig. 2 shows, for $N = 10$, the first derivative of the charge density, which is proportional to the distortive force, and the calculated change in atomic layer spacing. All of these quantities exhibit damped oscillations at a wavelength of $\lambda_F/2 = 1.98$ Å, which is close to two-thirds of the expected bulk interlayer spacing of 2.84 Å. Every two layers of Pb will thus roughly correspond to an integral number of oscillations in the charge density, resulting in an approximate bilayer periodicity of the lattice distortion. The quasi-bilayer periodicity in the film structure is most obvious in the layer relaxations near the surface, where the layers alternate between expansion and contraction (bottom panel of Fig. 2). In addition, the interlayer spacing between the two Pb layers of the film closest to the silicon substrate shows a substantial expansion, which is not easily accessible by other experimental techniques. Layer relaxation profiles for other thicknesses are qualitatively similar.

The x-ray diffraction results presented in this study show that the internal structure of thin metal films can be significantly modified as a result of quantum confinement and interference effects. Although smooth, 2-D films were studied in this experiment, it is reasonable to expect a similar phenomenon for 3-D nano-objects as well. An important finding from this experiment, however, is that the structural modifications due to such quantum size effects can penetrate many layers into the object and occur at all of its boundaries. Such effects must therefore be accounted for and considered in the design and applications of metallic nanoscale objects.

Acknowledgments

This work is supported by the U.S. Department of Energy (DOE) under Grant No. DEFG02-91ER45439. UNI-CAT is supported by the MRL at UIUC (DOE; State of Illinois Board of Higher Education, Higher Education Cooperation Act; and National Science Foundation [NSF]); Oak Ridge National Laboratory (DOE under contract with UT-Battelle, LLC); National Institute of Standards and Technology (U.S. Department of Commerce); and UOP LLC. The APS is supported by the DOE Office of Science, Office of Basic Energy Sciences, under Contract No. W-31-109-ENG-38. We also acknowledge partial equipment and personnel support from the Petroleum Research Fund, administered by the American Chemical Society, and from the NSF under Grant No. DMR-02-03003.

References

[1] P.J. Feibelman, Phys. Rev. B **27**, 1991 (1983).
[2] W.B. Su, S.H. Chang, W.B. Jian, C.S. Chang, L.J. Chen, and T.T. Tsong, Phys. Rev. Lett. **86**, 5116 (2001).
[3] A. Crottini, D. Cvetko, L. Floreano, R. Gotter, A. Morgante, and F. Tommasini, Phys. Rev. Lett. **79**, 1527 (1997).
[4] J. Braun and J.P. Toennies, Surf. Sci. **384**, L858 (1997).
[5] J.A. Carlisle, T. Miller, and T.-C. Chiang, Phys. Rev. B **45**, 3400 (1992).
[6] F. Grey, R. Feidenhans'l, M. Nielsen, and R.L. Johnson, Colloque de Physique **C7**, 181 (1989).
[7] M. Hupalo, V. Yeh, L. Berbil-Bautista, S. Kremmer, E. Abram, and M.C. Tringides, Phys. Rev. B **64**, 155307 (2001).
[8] B.E. Warren, *X-ray Diffraction* (Dover Publications, Mineola, N.Y., 1969).
[9] I.K. Robinson and E. Vlieg, Surf. Sci. **261**, 123 (1992).
[10] E.D. Specht and F.J. Walker, J. Appl. Crystallogr. **26**, 166 (1993).